# THE ACOUSTIC AND INSTABILITY WAVES OF JETS CONFINED INSIDE AN ACOUSTICALLY LINED RECTANGULAR DUCT

F. Q. Hu

Department of Mathematics and Statistics, Old Dominion University, Norfolk, Virginia 23529, U.S.A.

(Received 18 November 1993, and in final form 16 May 1994)

An analysis of linear wave modes associated with supersonic jets confined inside an acoustically lined rectangular duct is presented. Mathematical formulations are given for the vortex-sheet model and the continuous mean flow model of the jet flow profiles. Detailed dispersion relations of these waves in a two-dimensional confined jet as well as an unconfined free jet are computed. Effects of the confining duct and the liners on the jet instability and acoustic waves are studied numerically. It is found that the effect of the liners is to attenuate waves that have supersonic phase velocities relative to the ambient flow. The attenuation, however, is less effective for waves that have a subsonic phase velocity relative to the ambient flow. Numerical results also show that the growth rates of the instability waves could be reduced significantly by the use of liners. In addition, it is found that the upstream-propagating neutral waves of an unconfined jet could become attenuated when the jet is confined.

#### 1. INTRODUCTION

The exceedingly high level of jet noise presents a formidable barrier in developing future generation high speed civil transport planes (see, e.g., Seiner [1]). In a proposed scheme of jet noise reduction, the exit jet of the engine is guided through a rectangular duct before being discharged into the air. In the design concept, the purpose of the duct is twofold. First, cold air could be sucked into the duct by the hot jet through the side inlets and thus cool the jet stream and enhance the mixing. Second, the duct walls, installed with sound absorbing liners, could absorb a substantial part of the jet noise. Hence, it is important to understand and predict the generation, propagation and attenuation of jet noise inside a duct with sound absorbing liners. Furthermore, recent studies of supersonic jet noise generation mechanisms have indicated that the growth of the instability waves of the jet is responsible for the dominant part of the jet noise (see, e.g., Tam and Burton [2]). In view of these recent studies, it is important to re-examine the jet instabilities with the confining lined walls.

Duct acoustics and wave attenuation by wall liners have been investigated extensively in the literature (see the reviews by Nayfeh et al. [3] and Eversman [4], and the references cited therein). Pridmore-Brown [5] first formulated the acoustic wave propagation problem in an attenuating duct with non-uniform mean flows. However, due to computational limitations, most of the early works have only considered duct flows with uniform mean velocity and temperature distributions. Later, with increased computing power, the effects of the shear flow induced by the boundary layers at the duct walls were included in the acoustic wave attenuation calculations. In most studies, the shear flow of the boundary layer was approximated by a linear profile. It was found that the shear flow had a

refraction effect on the wave propagations. It was also shown that solutions with a thin boundary layer converge to that of a uniform mean flow, provided correct boundary conditions were used in the latter (Eversman and Beckemeyer [6]). Most recently, Bies *et al.* [7] presented a study that takes into account the coupled effects of the acoustic waves inside the duct and those in the liners. However, historically, little attention has been paid to the instabilities of the shear flow inside the duct and its impact on the sound generation.

Recently, the instability and acoustic waves associated with a planar mixing layer inside a rectangular duct have been studied by Tam and Hu [8]. In that work, the main interest was in the instability of a confined mixing layer at supersonic velocities. It was found that the instabilities of confined shear flows are quite different from those of their unconfined counterparts at high speeds. Systematic calculations of normal mode solutions showed that new instability wave modes are induced by the coupled effect of the acoustic modes of the confining duct and the instability of the shear layer. It was also shown that, at supersonic convective Mach numbers, acoustic waves that have supersonic phase velocities relative to both sides of the shear layer could be unstable (or amplified). The acoustic-mode instability of supersonic shear flows has also been found by Mack [9] for boundary layers and wakes, and for supersonic jets by Tam and Hu [10]. These studies have also shown that, at high supersonic speed, the acoustic-mode instability becomes the dominant flow instability.

In this paper, a detailed analysis is carried out of the linear wave modes, including the acoustic waves and instability waves, associated with a given non-uniform mean flow inside a rectangular duct with finite wall impedance. The numerical results presented here are, however, limited to two-dimensional waves. Two models of the jet flow, a vortex-sheet model and a continuous mean flow model, will be used. In section 2, the mathematical formulation of the problems is given. In Section 3 the numerical results are presented. Section 4 contains the concluding remarks.

### 2. FORMULATIONS

#### 2.1. MATHEMATICAL MODELS

Small amplitude waves are considered, associated with a given mean flow of a jet profile inside a rectangular duct (Figure 1). Here the mean velocities and densities of the jet core and the ambient stream will be denoted by  $u_j$ ,  $\rho_j$  and  $u_a$ ,  $\rho_a$ , respectively. The jet exit has a width of 2d. The height of the duct is denoted by 2h and the width by B. The top and bottom walls of the duct are lined with acoustically treated materials with finite acoustic impedance. Two side walls are taken to be solid walls. For simplicity, it is assumed that

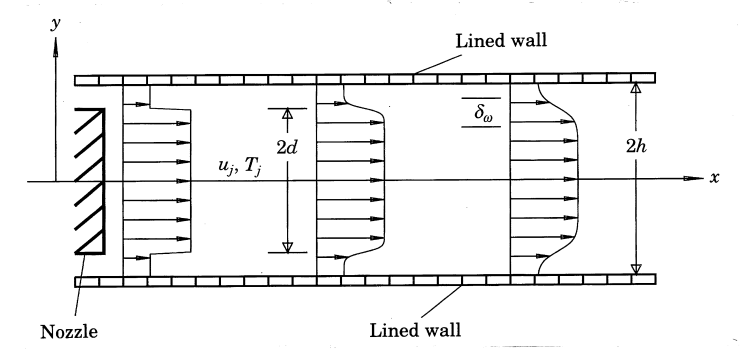


Figure 1. A schematic of a confined jet with lined walls. The jet width is 2d, and the duct height is 2h. The vorticity thickness of the mean velocity is  $\delta_{\omega}$ .

the top and bottom walls are lined with the same materials. From linear stability considerations, the locally parallel flow assumption will be used throughout their study. To facilitate the numerical investigation, two models of the mean flow will be used in the present paper. In the first model, here referred to as the vortex-sheet model, the mean flow is piecewise uniform for the velocity and temperature. This profile models the flow just downstream of the jet nozzle near the nozzle exit. The advantage of the vortex-sheet model is that a closed form dispersion equation can be found. This allows for an extensive numerical study about the nature of all the wave modes. In the second model the mean flow is continuous. This permits more realistic flows and models the flow further downstream of the jet nozzle exit.

#### 2.2. GOVERNING EQUATIONS AND BOUNDARY CONDITIONS

Each flow variable can be expressed as a mean quantity plus a small perturbation, as follows:

$$\begin{pmatrix} u(x, y, z, t) \\ v(x, y, z, t) \\ w(x, y, z, t) \\ p(x, y, z, t) \\ \rho(x, y, z, t) \end{pmatrix} = \begin{pmatrix} \bar{u}(y) \\ 0 \\ 0 \\ \bar{p} \\ \bar{\rho}(y) \end{pmatrix} + \begin{pmatrix} u'(x, y, z, t) \\ v'(x, y, z, t) \\ w'(x, y, z, t) \\ p'(x, y, z, t) \\ \rho'(x, y, z, t) \end{pmatrix}.$$

In the above, the x co-ordinate is in the downstream direction, y is in the vertical direction and z is in the spanwise direction. u, v and w are the velocities in the x, y and z directions, respectively, p is the pressure and p is the density. An overbar indicates the mean quantity and prime indicates the perturbation. It is straightforward to find that the linearized governing equations for inviscid, non-heat-conducting fluids are

$$\frac{\partial \rho'}{\partial t} + \bar{u}\frac{\partial \rho'}{\partial x} + \frac{\mathrm{d}\bar{\rho}}{\mathrm{d}y}v' + \bar{\rho}\left(\frac{\partial u'}{\partial x} + \frac{\partial v'}{\partial y} + \frac{\partial w'}{\partial z}\right) = 0,\tag{1}$$

$$\frac{\partial u'}{\partial t} + \bar{u}\frac{\partial u'}{\partial x} + \frac{\mathrm{d}\bar{u}}{\mathrm{d}y}v' = -\frac{1}{\bar{\rho}}\frac{\partial p'}{\partial x}, \qquad \frac{\partial v'}{\partial t} + \bar{u}\frac{\partial v'}{\partial x} = -\frac{1}{\bar{\rho}}\frac{\partial p'}{\partial y}, \qquad (2,3)$$

$$\frac{\partial w'}{\partial t} + \bar{u}\frac{\partial w'}{\partial x} = -\frac{1}{\bar{\rho}}\frac{\partial p'}{\partial z}, \qquad \frac{\partial p'}{\partial t} + \bar{u}\frac{\partial p'}{\partial x} + \gamma \bar{p}\left(\frac{\partial u'}{\partial x} + \frac{\partial v'}{\partial y} + \frac{\partial w'}{\partial z}\right) = 0. \tag{4, 5}$$

The temperature T is related to the pressure and density by the equation of state:

$$p = \rho RT. \tag{6}$$

For the system (1)–(5), solutions are sought of the form

$$\begin{pmatrix}
u'(x, y, z, t) \\
v'(x, y, z, t) \\
w'(x, y, z, t) \\
p'(x, y, z, t) \\
\rho'(x, y, z, t)
\end{pmatrix} = \begin{pmatrix}
\hat{u}(y) \cos(2\pi mz/B) \\
\hat{v}(y) \cos(2\pi mz/B) \\
\hat{w}(y) \sin(2\pi mz/B) \\
\hat{p}(y) \cos(2\pi mz/B) \\
\hat{\rho}(y) \cos(2\pi mz/B)
\end{pmatrix} e^{i(kx - \omega t)}, \tag{7}$$

Substituting equation (7) into equations (1)–(5), together with the proper boundary conditions, an eigenvalue problem is formed. The eigensolutions will be called the "normal modes", as in hydrodynamic stability theory. In equation (7), the boundary conditions at the two solid side walls, located at  $\bar{z} = \pm B/2$ , are satisfied automatically. At the acoustically treated top and bottom walls, located at  $y = \pm h$ , the kinematic boundary

condition is the continuity of particle displacement at the lined walls. For harmonic waves, it yields (see, e.g., Nayfeh *et al.* [3])

$$\hat{v} = -\frac{(k\bar{u} - \omega)}{\omega Z}\hat{p},\tag{8}$$

where Z is the wall impedance  $(Z = p_{wall}/v_{wall})$ .

In equation (7), m is a modal number indicating wave reflections in the z direction. When m=0, the waves are two-dimensional. Only two-dimensional waves will be calculated in this paper. The mathematical formulation of the eigenvalue problems for the vortex-sheet model and the continuous mean flow profile model is given below.

#### 2.3. VORTEX-SHEET MODEL

For the vortex-sheet model, the jet boundaries are represented by infinitely thin vortex sheets. Thus, the mean flow is piecewise uniform and a closed form dispersion equation can be found. In addition, due to the symmetry of the mean flow, it is convenient to consider symmetric  $(d\hat{p}(0)/dy = 0)$  and antisymmetric  $(\hat{p}(0) = 0)$  wave modes separately. As a result, only the flow in the upper half of the duct needs to be considered. By satisfying the boundary conditions at the wall, equation (8), and the jet interface (i.e., the continuity of pressure and particle displacement), the dispersion equation which implicitly relates  $\omega$  and k is found as follows. For symmetric modes,

$$\frac{\lambda_{j} \tan (\lambda_{j} d)}{\rho_{j} (\omega - k u_{j})^{2}} - \frac{\lambda_{a}}{\rho_{a} (\omega - k u_{a})^{2}} \frac{\rho_{a} (\omega - k u_{a})^{2} \cos \left[\lambda_{a} (h - d)\right] - i\omega \lambda_{a} Z \sin \left[\lambda_{a} (h - d)\right]}{\rho_{a} (\omega - k u_{a})^{2} \sin \left[\lambda_{a} (h - d)\right] + i\omega \lambda_{a} Z \cos \left[\lambda_{a} (h - d)\right]} = 0; (9a)$$

and for antisymmetric modes,

$$\frac{\lambda_{j}\cot(\lambda_{j}d)}{\rho_{j}(\omega-ku_{j})^{2}} + \frac{\lambda_{a}}{\rho_{a}(\omega-ku_{a})^{2}} \frac{\rho_{a}(\omega-ku_{a})^{2}\cos\left[\lambda_{a}(h-d)\right] - i\omega\lambda_{a}Z\sin\left[\lambda_{a}(h-d)\right]}{\rho_{a}(\omega-ku_{a})^{2}\sin\left[\lambda_{a}(h-d)\right] + i\omega\lambda_{a}Z\cos\left[\lambda_{a}(h-d)\right]} = 0; (9b)$$

where

$$\lambda_a = \sqrt{[(\omega - ku_a)/c_a]^2 - k^2 - (2m\pi/B)^2}, \qquad \lambda_j = \sqrt{[(\omega - ku_j)/c_j]^2 - k^2 - (2m\pi/B)^2},$$
 and the speeds of sound are given by  $c_{a,j} = \sqrt{\gamma p/\rho_{a,j}}$ .

Here, it is interesting to note two special cases of the dispersion equations given above; i.e., when the mean flow is uniform and when the duct walls are solid boundaries.

## 2.3.1. Uniform mean flow

For a uniform flow profile inside the duct,  $u_a = u_j$ ,  $\rho_a = \rho_j$  and d = h. The dispersion relations, equations (9a) and (9b), then become

$$\tan (\lambda_i d) - \rho_i (\omega - k u_i)^2 / \mathrm{i} \omega \lambda_i Z = 0$$

for symmetric modes and

$$\cot (\lambda_i d) + \rho_i (\omega - k u_i)^2 / \mathrm{i} \omega \lambda_i Z = 0$$

for antisymmetric modes, respectively. The above two equations are the same as those obtained in the literature for uniform mean flows (Nayfeh et al. [3]).

## 2.3.2. Solid walls

For solid walls,  $Z \rightarrow \infty$ . In this case, the dispersion relations, equation (9a) and (9b), reduce to

$$\frac{\lambda_j \tan (\lambda_j d)}{\rho_j (\omega - k u_j)^2} + \frac{\lambda_a \tan [\lambda_a (h - d)]}{\rho_a (\omega - k u_a)^2} = 0$$

for symmetric modes (Tam and Hu [8]) and

$$\frac{\lambda_j \cot (\lambda_j d)}{\rho_j (\omega - k u_j)^2} - \frac{\lambda_a \tan \left[\lambda_a (h - d)\right]}{\rho_a (\omega - k u_a)^2} = 0$$

for antisymmetric modes, respectively.

#### 2.4. CONTINUOUS MEAN FLOW MODEL

For continuous mean flow profiles, upon substituting equation (7) into equations (1)–(5), the linearized governing equations can be reduced to a single equation for the pressure perturbation:

$$\frac{\mathrm{d}^2 \hat{p}}{\mathrm{d}y^2} + \left(\frac{2k}{\omega - k\bar{u}} \frac{\mathrm{d}\bar{u}}{\mathrm{d}y} - \frac{1}{\hat{\rho}} \frac{\mathrm{d}\hat{\rho}}{\mathrm{d}y}\right) \frac{\mathrm{d}\hat{\rho}}{\mathrm{d}y} + \left[\left(\frac{\omega - k\bar{u}}{\bar{c}}\right)^2 - k^2 - \left(\frac{2m\pi}{B}\right)^2\right] \hat{p} = 0, \tag{10}$$

where  $\bar{c}$  is the speed of sound.

The boundary conditions for  $\hat{p}$  are, at y = h,

$$\hat{p} + \frac{\mathrm{i}\omega Z}{\bar{\rho}_a(\omega - k\bar{u}_a)^2} \frac{\mathrm{d}\hat{p}}{\mathrm{d}y} = 0,\tag{11}$$

and, at y = 0,

$$d\hat{p}/dy = 0$$
 (symmetric modes) or  $\hat{p} = 0$  (antisymmetric modes). (12a, b)

Equation (10) and the boundary conditions (11) and (12) form an eigenvalue problem. The problem will be solved numerically by integrating from the centerline y=0 to the upper boundary y=h and employing a shooting method, using the results of the vortex-sheet model as the starting solutions. Similar numerical computations have been carried out in the past with non-uniform subsonic velocity profiles (e.g. Mungur and Gladwell [11] and Ko [12]; also see the references listed in references [3, 4]). Here, the emphasis is on the supersonic jet flow with instability waves.

#### 3. NUMERICAL RESULTS

For the numerical results shown below, the Mach numbers of the jet and ambient flow are  $M_j = 2.0$  and  $M_a = 0.2$ , respectively. The ratio of the speeds of sound  $c_a/c_j = 0.5$ . All the results shown are with respect to two-dimensional symmetric wave modes. Results of antisymmetric modes are similar and are not shown here.

#### 3.1. RESULTS OF THE VORTEX-SHEET MODEL

The main interest is to determine the normal modes associated with a two-dimensional supersonic jet confined inside a duct and study the effects of the confining lined walls on these wave modes. For the purpose of making comparisons, the dispersion relations of an *unconfined* jet will be discussed briefly.

## 3.1.1. Unconfined jets

The normal modes of a free circular jet have been studied extensively by Tam and Hu [10]. Here, some properties of a two-dimensional free jet will be examined briefly.

For a two-dimensional free jet, the dispersion equation relating the frequency  $\omega$  and wavenumber k is given by

$$\frac{\mathrm{i}\lambda_a \cos\left(\lambda_j d\right)}{\rho_a (\omega - k u_a)^2} + \frac{\lambda_j \sin\left(\lambda_j d\right)}{\rho_i (\omega - k u_i)^2} = 0 \tag{13a}$$

for the symmetric modes and

$$\frac{\mathrm{i}\lambda_a \sin\left(\lambda_j d\right)}{\rho_a (\omega - k u_a)^2} - \frac{\lambda_j \cos\left(\lambda_j d\right)}{\rho_j (\omega - k u_j)^2} = 0 \tag{13b}$$

for the antisymmetric modes (Gill [13]). The dispersion relation of the symmetric modes has been computed and is shown in Figure 2 ( $k_r$  and  $k_i$  are the real and imaginary parts of the wavenumber k, respectively). Numerical studies of the dispersion equation (13a) indicate that the present "top hat" jet profile possesses instability waves as well as neutrally stable acoustics waves. Furthermore, since the convective Mach number (here defined as  $M_c = (u_j - u_a)/(c_j + c_a)$ ) is greater than one in the present case, a family of supersonic instability waves is also present, in addition to the Kelvin–Helmholtz instability wave. This family of unstable modes have supersonic phase velocities relative to both the jet and ambient streams. The properties of these supersonic instability waves were more fully discussed by Tam and Hu [10].

In addition to the unstable wave modes, namely the K–H wave and the supersonic instability waves, there are also two families of neutrally stable waves associated with the free jet. Here, these two families are referred to as the family C and family D acoustic waves. For convenience of discussion, we divide the  $k_r - \omega$  plane into five regions by the sonic lines as indicated in the figure. Two aspects of the neutral acoustic waves are worth pointing out. First, we note that the neutral waves are found only in region I, above the

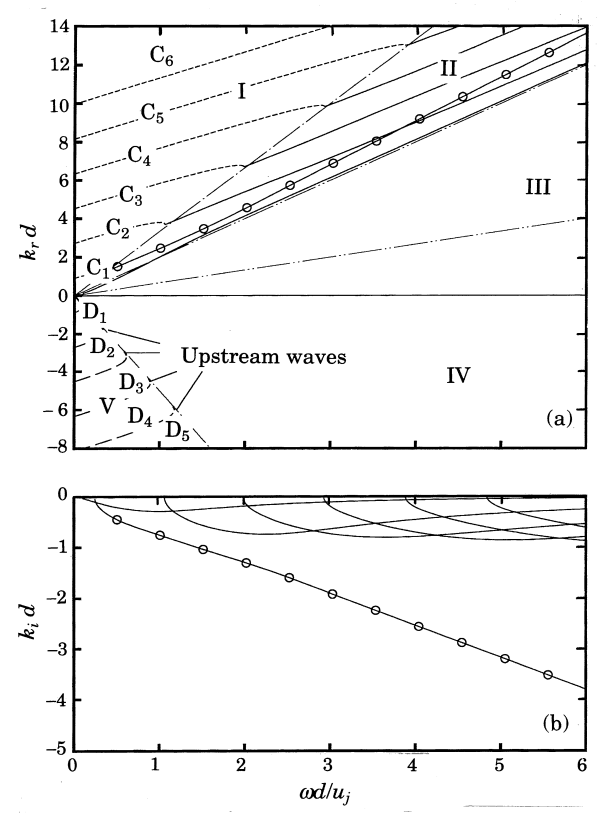


Figure 2.. The dispersion relation of an unconfined jet. The symmetric modes are shown. (a) Real; (b) imaginary.  $M_j = 2.0$ ,  $M_a = 0.2$ ,  $c_a/c_j = 0.5$ . —O—, Kelvin–Helmholtz mode; ——, supersonic instability modes; ----, family C modes; ----, family D modes; ----, sonic lines  $\omega/k_r = u_a \pm c_a$ ; — -----, sonic lines  $\omega/k_r = u_i \pm c_j$ .

sonic line  $\omega/k_r = u_a + c_a$ , or in region V, below the sonic line  $\omega/k_r = u_a - c_a$ : That is, the phase velocity,  $C_{ph} = \omega/k$ , of the neutral wave is always subsonic relative to the ambient, i.e.,  $|C_{ph} - u_a| \le c_a$ . For class C waves,  $0 \le C_{ph} \le u_a + c_a$ ; and for class D waves,  $u_a - c_a \le C_{ph} \le 0$ . In other words, for the free jet, the neutral waves attached to the jet are necessarily decaying away from the jet. Second, it has been found that part of the class D waves represent upstream waves with a phase velocity close to  $u_a - c_a$ , as indicated in Figure 2 where the group velocities are negative (see also Tam and Hu [10]). This means that it is possible to have upstream-propagating neutral waves even though the jet mean velocity is supersonic. This point will be re-examined more closely later.

# 3.1.2. Confined jets

In this section the effects of the duct walls will be considered, and the normal modes associated with a confined jet will be computed. First, the case in which the duct walls are solid boundaries is considered. The case in which the duct walls are lined will be dealt with in section 3.1.3. For solid walls, let  $Z \to \infty$  in equation (9). With the vortex sheet model, the frequency and wavenumber of the wave modes are then the roots or zeros of the dispersion equations (9a) or (9b). In the present work, interest lies in the spatially attenuating or growing waves: thus,  $\omega$  will be a real number. However, for systems that have spatial instabilities, it is not sufficient to just set the frequency  $\omega$  to be a real number and look for the zeros of the dispersion equations in the complex k-plane. One must distinguish the downstream and upstream propagating waves. Without the proper distinction, a downstream-propagating growing wave may be erroneously considered as an upstream-propagating attenuating wave, and vice versa. For this reason, the criterion developed by Briggs [14] and also used by Tam and Hu [8] will be followed here. In this procedure, the frequency  $\omega$  is first given a complex number, the real part of which is the frequency of interest and the imaginary part of which is some large positive number. The corresponding zeros of the dispersion equation are found in the complex k-plane. Then an  $\omega$ -contour deformation process is applied, in which the real part of  $\omega$  is kept constant while the imaginary part of  $\omega$  is gradually reduced to zero. In this process, the corresponding zeros of the dispersion equation in the k-plane are traced as the imaginary part of  $\omega$  is reduced. In Briggs' criterion, the zeros originating from the upper half of the k-plane represent the downstream-propagating waves, and the zeros from the lower half of the k-plane represent the upstream-propagating waves.

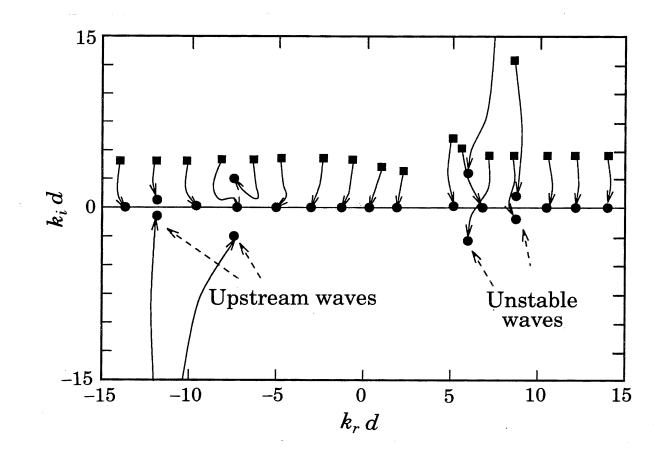


Figure 3. Trajectories of zeros of the dispersion equation in the complex k plane as  $\omega d/u_i$  is varied from 3 + 5i to 3. The symmetric modes with solid walls are shown.  $M_i = 2.0$ ,  $M_a = 0.2$ ,  $c_a/c_i = 0.5$ , d/h = 0.75.

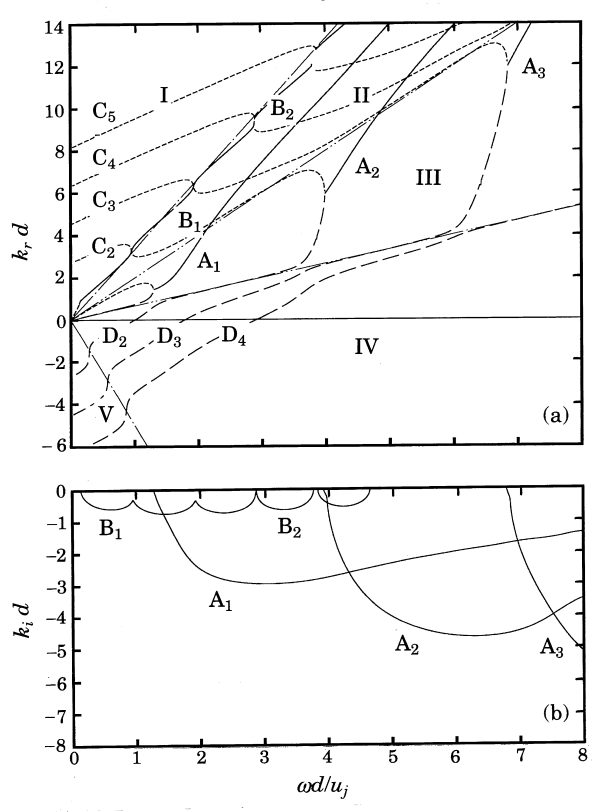


Figure 4. The dispersion relation of an confined jet. The symmetric modes are shown. (a) Real; (b) imaginary.  $M_j = 2.0$ ,  $M_a = 0.2$ ,  $c_a/c_j = 0.5$ , d/h = 0.75, solid walls at  $y = \pm h$ . —, Unstable modes; ----, family D modes; ----, sonic lines  $\omega/k_r = u_a \pm c_a$ ; -----, sonic lines  $\omega/k_r = u_j \pm c_j$ .

To illustrate the above process, the traces of the zeros in the k-plane as the imaginary part of  $\omega$  is being reduced are plotted in Figure 3 for the case of Re  $(\omega d/u_j) = 3$ . The propagation direction of the wave mode associated with each zero in the k-plane is correctly identified according to its movement in the process. Those zeros that move across the real k-axis will represent instability waves. Those zeros that remain in the upper or lower half of the k-plane then represent decaying or attenuated waves. Moreover, zeros that lie on the real k-axis in Figure 3 represent the neutrally stable acoustic waves.

The above procedure has been applied systematically as the real part of the  $\omega$  changes. The dispersion relations so obtained are given in Figure 4. (A similar procedure has been used in the free jet calculations given in the previous section.) For convenience of discussion, wave modes have been classified into two families of unstable waves, and A and B modes, and two families of neutrally stable acoustic waves, the C and D waves. However, a detailed description of the characteristics of each family of waves will not be given here. They are quite similar to the four families previously found in a planar mixing layer (Tam and Hu [8]).

Now compare the dispersion relation of the confined jet given in Figure 4 with that of an unconfined free jet shown in Figure 2. First note that, due to the confinement, the neutral waves can have a phase speed supersonic to the ambient flow. The dispersion relation curves for family C and family D neutral waves now extend across the sonic lines  $C_{ph} = u_a \pm c_a$  continuously.

Furthermore, upon closer inspection of Figure 4, the dispersion relation diagram shows that the family D waves now all have positive group velocities. To study the upstream waves, the real and imaginary parts of k as functions of  $\omega$  are plotted in Figure 5 for the first three zeros that originate from the lower half of the k-plane in the contour deformation process. It is seen that although these wavenumbers have negative imaginary parts, they are actually attenuating waves, as they are upstream-propagating waves. Careful numerical computations show that for  $\omega d/u_j < 4$ , no zero reaches the real k-axis from below. In other words, low frequency upstream-propagating waves of the free jet are attenuated due to the presence of the confining walls.

Since the upstream-propagating waves of the unconfined jet have phase velocities close to  $u_a - c_a$  in the unconfined jets (see Figure 2), we now calculate the group velocity,  $\partial \omega/\partial k$ , for neutral waves along the sonic line  $C_{ph} = u_a - c_a$ . By letting  $\omega/k = u_a - c_a$ , the derivative  $\partial \omega/\partial k$  can be obtained analytically from the dispersion equations given by equations (9a) and (9b). For reasons of brevity, the expression for  $\partial \omega/\partial k$  is not given here. To have neutral waves that travel upstream, it is necessary that  $\partial \omega/\partial k < 0$ . It is found that, for both the symmetric and antisymmetric modes, this requires that

$$\frac{h-d}{d} > \frac{c_a u_j (u_j + c_a - u_a) - c_j^2 c_a}{2(c_a - u_a)(u_j + c_a - u_a)^2},$$

or in non-dimensional parameters,

$$\frac{h-d}{d} > \frac{M_j[M_j + (1-M_a)(c_a/c_j)] - 1}{2(1-M_a)[M_j + (1-M_a)(c_a/c_j)]^2}.$$
(14)

The boundary curves in the space  $M_j$  versus d/h for different ambient Mach numbers are plotted in Figure 6. Asymptotically, for hot jets and a low Mach number in the ambient, the upstream waves are attenuated when d/h > 2/3. For cold jets, this condition is d/h > 3/4.

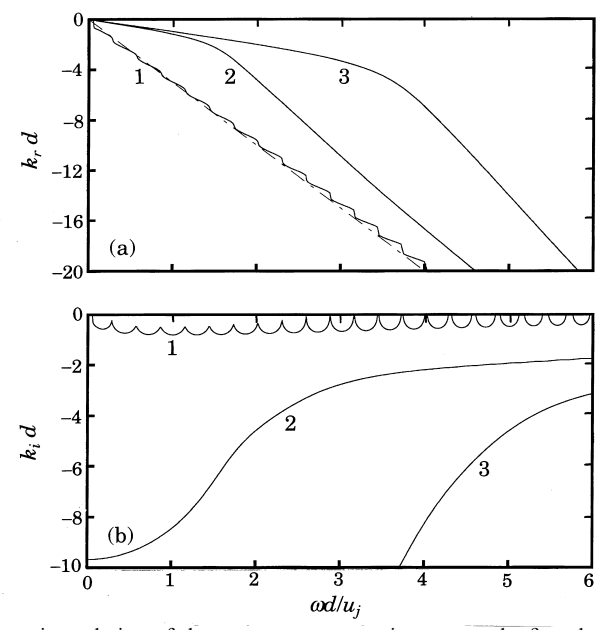


Figure 5. The dispersion relation of the upstream-propagating waves; the first three zeros originating in the lower half of the k-plane are shown. (a) Real; (b) imaginary.  $M_j = 2.0$ ,  $M_a = 0.2$ ,  $c_a/c_j = 0.5$ , d/h = 0.75, solid walls.

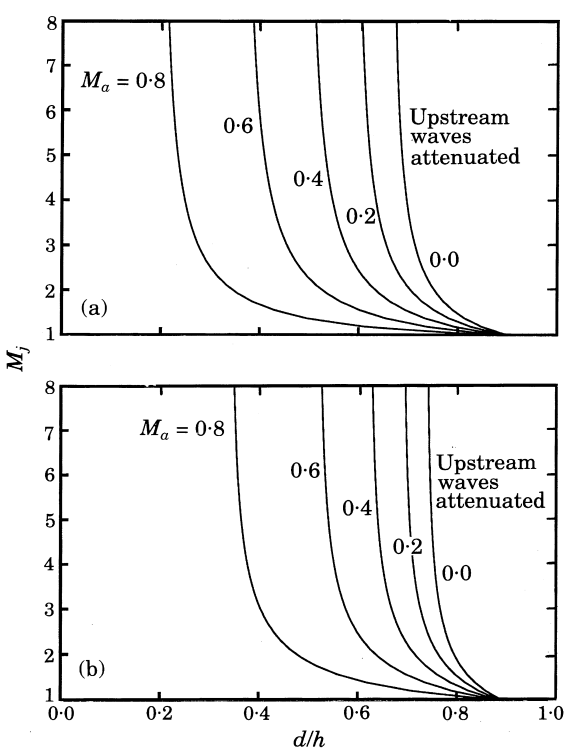


Figure 6. Boundaries for attenuation of the upstream-propagating waves. (a) Hot jet,  $T_i/T_a = 4$ ; (b) cold jet.

#### 3.1.3. Effects of wall liners

The effects of the finite wall impedance of the liners on the acoustic and the instability waves discussed in the previous section are now studied. A point-reacting wall impedance model will be used in the present study [3]. In this model, the impedance of the wall is given by

$$Z = \rho_a c_a [R + i \cot(\omega l/c_a)], \tag{15}$$

where  $\rho_a$  and  $c_a$  are the density and speed of sound of the ambient fluid, l is the thickness of the liner cavity and R is the resistance (non-dimensional) of the wall facing the flow. In all the results reported below, l = 0.05h and R varies.

Numerical calculations show that the liner effect varies for waves in different regions in the dispersion diagram. For instance, for the acoustic waves in regions I and V, the phase velocity is subsonic relative to the ambient flow but supersonic relative to the jet. These waves are trapped inside the jet and their eigenfunctions decay away from the jet. The effect of the liner has been found to be minimal. On the other hand, for acoustic waves in regions II, III and IV, the phase velocity is supersonic relative to the ambient flow. Their eigenfunctions show a larger pressure perturbation at the wall. A larger influence of the liner has been found on the wave modes in these regions. This is demonstrated in Figure 7, in which eigenfunctions of selected wave modes for solid and lined walls are plotted. Also plotted are the eigenfunctions of A and B instability wave modes. In particular, for family A waves, the eigenfunction has a peak at the jet boundary, y = 0.75h, and decays towards the wall. Thus, the effects of the lined walls are not significant. For the B modes, however, the eigenfunction decays slowly towards the wall. For this family of waves, a larger effect of the lined walls was shown.

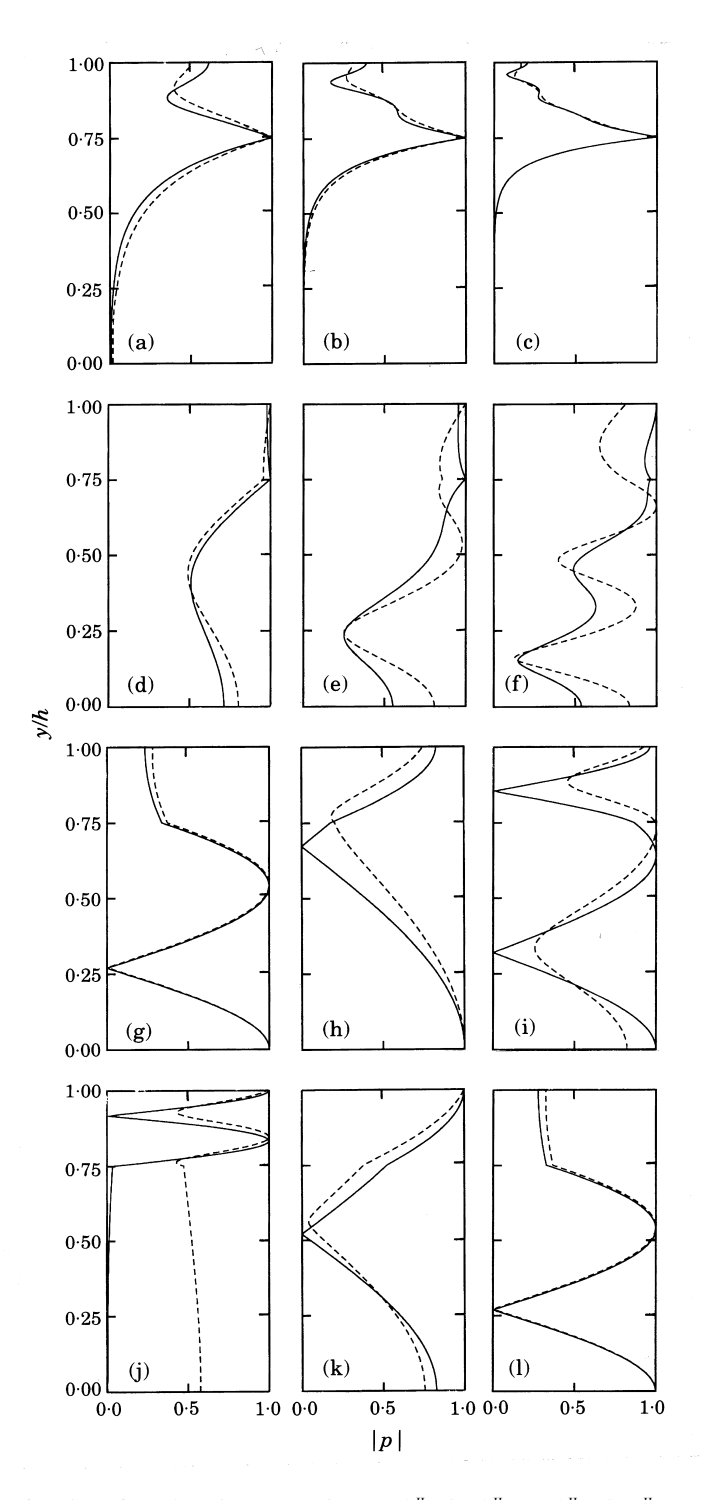


Figure 7. Eigenfunctions for selected wave modes. (a)  $A_1^{II}$ ; (b)  $A_2^{II}$ ; (c)  $A_3^{II}$ ; (d)  $B_1^{II}$ ; (e)  $B_2^{II}$ ; (f)  $B_3^{II}$ ; (g)  $C_2^{II}$ ; (h)  $C_2^{II}$ ; (i)  $C_3^{II}$ ; (j)  $D_2^{III}$ ; (k)  $D_2^{IV}$ ; (l)  $D_2^{V}$ . —, Solid walls; ----, lined walls with R=2. Superscripts indicate the regions of the wave mode in Figure 4. Symmetric modes,  $M_j=2.0$ ,  $M_a=0.2$ ,  $C_a/C_j=0.5$ , d/h=0.75.

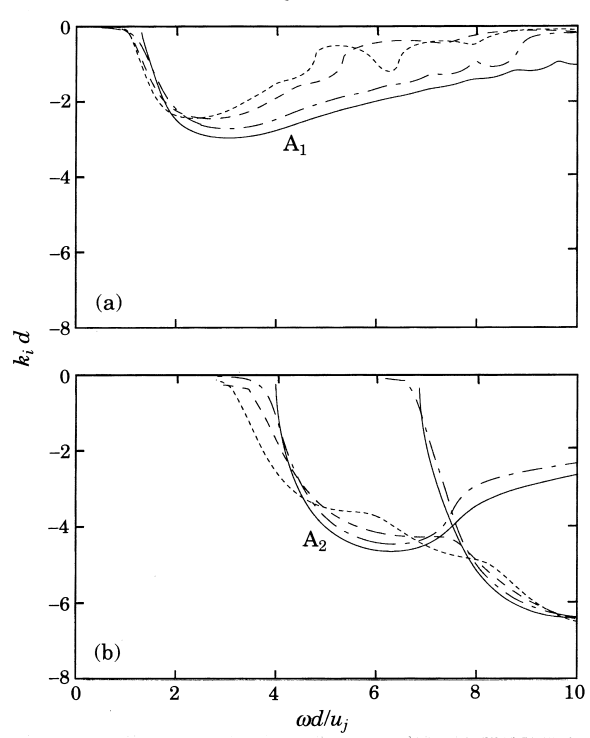


Figure 8. The effects of liners in the growth rates. (a)  $A_1$  mode; (b)  $A_2$  and  $A_3$  modes. ——, Solid walls; -----, R = 5; ----, R = 2; -----, R = 1. Symmetric modes,  $M_j = 2 \cdot 0$ ,  $M_a = 0 \cdot 2$ ,  $C_a/C_j = 0 \cdot 5$ ,  $C_a/C_j$ 

In Figure 8 are shown the effects of the acoustic liner on the growth rates of the instability waves: plotted are the spatial growth rates of the first three family A waves for wall resistance R = 1, 2 and 5 respectively. Clearly, the growth rates are reduced when finite impedance walls are used. However, it must also be pointed out that the attenuation effects are not significant for second and third modes, namely the  $A_2$  and  $A_3$  modes.

In Figure 9, the effects of the liners on the acoustic modes are shown: plotted are the imaginary parts of the complex wavenumber as functions of 1/R. It is seen that with lined walls, the family D waves are attenuated but the family C waves are actually destablized. Further investigations have indicated that this destablization is a direct result of a merging of the C and the unstable B waves when the impedance Z becomes complex in the dispersion relation (9). Again, it is clear from Figure 9 that the degree of influence of the liners on the acoustic waves depends largely on the phase velocity of the waves and thus the region in the dispersion diagram. The least affected are the waves in regions I and V, in which the phase velocity of the wave is subsonic relative to the ambient flow.

## 3.2. RESULTS OF THE CONTINUOUS MEAN FLOW MODEL

For the continuous mean flow model, a hyperbolic tangent function has been used for the mean velocity profile, namely,

$$\bar{u}(y) = \frac{1}{2}(\bar{u}_a + \bar{u}_i - (\bar{u}_a - \bar{u}_i) \tanh [2(|y| - d)/\delta_{\omega}]),$$

and the mean temperature profile obtained from Crocco's relation (Hu [15]). Here,  $\delta_{\omega}$  represents the vorticity thickness of the shear layer, defined as

$$\delta_{\omega} = |\bar{u}_i - \bar{u}_a|/(\partial \bar{u}/\partial v)_{max}$$
.

853

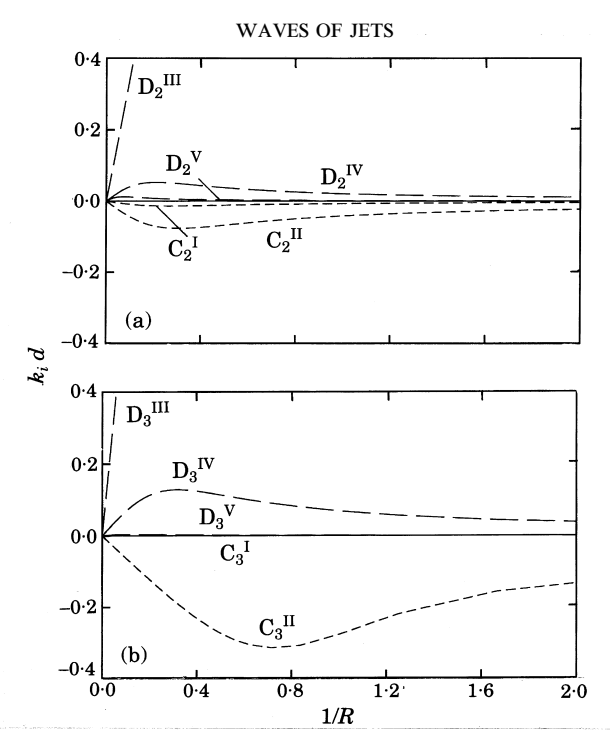


Figure 9.  $k_i$  as a function of 1/R for the C and D wave modes. (a) C<sub>2</sub> and D<sub>2</sub> modes; (b) C<sub>3</sub> and D<sub>3</sub> modes. Superscripts indicate the regions of the wave mode in Figure 4. Symmetric modes,  $M_j = 2.0$ ,  $M_a = 0.2$ ,  $c_a/c_j = 0.5$ , d/h = 0.75.

In the vortex-sheet model, the jet boundary is infinitely thin and the vorticity thickness is zero. As the vorticity thickness increases and becomes finite (i.e., greater than zero), the mean velocity and temperature profiles are continuous across the jet boundary. In this study with the finite thickness mean velocity profile, emphasis will be placed on the liner

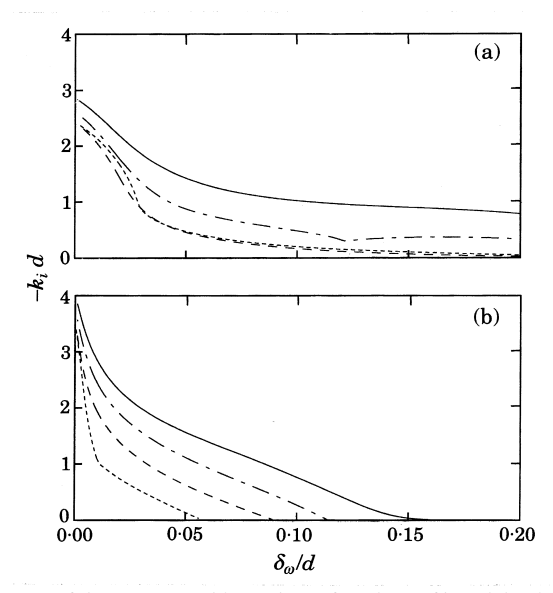


Figure 10. The growth rates of the most unstable modes as functions of jet mixing layer thickness. (a)  $A_1$  mode; (b)  $A_2$  mode. ——, Solid walls; ----, R = 5; ----, R = 2; ----, R = 1. Symmetric modes,  $M_j = 2.0$ ,  $M_a = 0.2$ ,  $C_a/C_j = 0.5$ , d/h = 0.75.

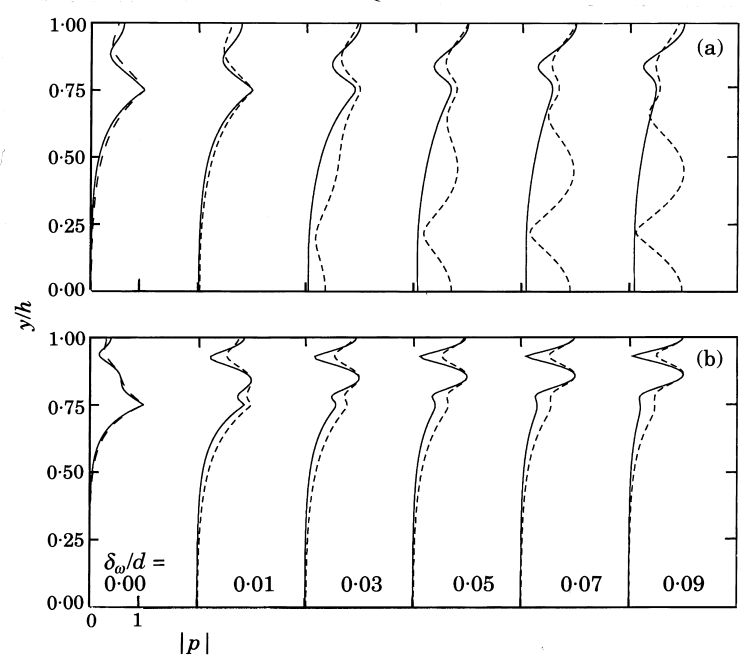


Figure 11. The eigenfunctions of the most unstable modes as thickness varies. (a)  $A_1$  mode; (b)  $A_2$  mode. —, Solid wall; ----, R=2.

effects on the instability waves. In particular, only the family A instability waves will be examined here, since they have larger growth rates than the family B modes.

In Figure 10, the growth rate  $(-k_id)$  as a function of the vorticity thickness is given for the most amplified  $A_1$  and  $A_2$  modes. Calculations were made for both the solid and lined walls. In general, as the thickness of the jet shear layer increases, the growth rate of the instability waves decreases. However, it is clear from the results shown that the liner becomes more effective in reducing the growth rates of the instability wave when finite thickness effects are considered. In Figure 11, the variation of the eigenfunctions is shown as the thickness of the jet shear layer increases. It is seen that, as the thickness increases, the relative peak of the eigenfunction at the jet boundary is reduced. As a result, the influence of the wall boundary condition increases. Based on the results shown, for a realistic jet flow with a finite vorticity thickness, say  $\delta_{\omega} > 0.05d$ , the acoustic liner can reduce the growth rate of the instability waves quite signficantly.

## 4. CONCLUDING REMARKS

A detailed analysis of the linear wave modes associated with a jet confined inside acoustically lined duct walls has been carried out. The dispersion relations of the acoustic and instability waves have been computed and given for the two-dimensional modes. The effects of the confining walls and the linears on the linear waves of the jet have been studied. It is found that the effect of the linears is to attenuate waves that have supersonic phase velocities relative to the ambient flow. However, the attenuation is less effective for the waves that have a subsonic phase velocity relative to the ambient flow. In addition, it is found that due to the presence of the confining walls, the upstream-propagating waves associated with a free supersonic jet could become attenuated under conditions given by equation (14). Furthermore, it is shown that, with a finite shear layer thickness, the acoustic

liners have a quite significant effect in reducing the growth rates of the instability waves of the jet.

In recent studies on supersonic jet noise generation mechanisms [2], the growth of the instability waves of the jet plays a central role in the noise generation. The results of the present study indicate that growth rates of the instability waves could be reduced greatly by employing lined walls. It is then reasonable to expect that this reduction in the growth rate of the instability waves may not only result in a change in the hydrodynamics (spreading rate and turbulent structures) but also result in a change in the noise generation of the jet. Moreover, in recent studies of jet screech tone noises, it has been suggested that the upstream-propagating wave of the free jet is an essential part of a feedback mechanism (see Tam and Norum [16] and Tam *et al.* [17]). The present study, however, shows that these upstream-propagating waves could become attenuated due to the confinement of the jet. It will be interesting and challenging further to examine and explore the direct consequences of these wave propagation properties on the noise generation. However, this is beyond the scope of the present study.

#### ACKNOWLEDGMENTS

The author wishes to thank Drs W. E. Zorumski, W. Watson and T. L. Jackson for many helpful discussions. The author also wishes to thank the reviewers for helpful suggestions. This work was supported by the National Aeronautics and Space Administration under NASA Contract NAS1-19480, while the author was in residence at the Institute for Computer Applications in Science and Engineering, NASA Langley Research Center, Hampton, Virginia 23665, U.S.A.

#### REFERENCES

- 1. J. M. Seiner 1992 *Studies in Turbulences*, 297–323. Berlin: Springer-Verlag. Fluid dynamics and noise emission associated with supersonic jets.
- 2. C. K. W. TAM and D. E. Burton 1984 *Journal of Fluid Mechanics* 138, 273–295. Sound generated by instability waves of supersonic flows, part 2: axisymmetric jets.
- 3. A. H. NAYFEH, J. E. KAISER and D. P. TELIONIS 1975 American Institute of Aeronautics and Astronautics Journal 13, 130–153. Acoustics of aircraft engine-duct systems.
- 4. W. Eversman 1991 Aeroacoustics of Flight Vehicles: Theory and Practice, NASA RP 1258, Vol. 2, 101–163. Theoretical modes for duct acoustic propagation and radiation.
- 5. D. C. Pridmore-Brown 1958 *Journal of Fluid Mechanics* **4**, 393–406. Sound propagation in a fluid flowing through an attenuating duct.
- 6. W. Eversman and H. E. Beckemeyer 1972 *Journal of the Acoustical Society of America* **52**, 216–220. Transmission of sound in ducts with thin shear layers-convergence to the uniform flow case
- D. A. BIES, C. H. HANSEN and G. E. BRIDGES 1991 Journal of Sound and Vibration 146, 47–80. Sound attenuation in rectangular and circular cross-section ducts with flow and bulk-reacting liners.
- 8. C. K. W. Tam and F. Q. Hu 1989 *Journal of Fluid Mechanics* **203**, 51–76. The instability and acoustic wave modes of supersonic mixing layers inside a rectangular channel.
- 9. L. M. MACK 1990 *Theoretical and Computational Fluid Dynamics* **2**, 97–123. On the inviscid acoustic-mode instability of supersonic shear flows, part 1: two-dimensional waves.
- 10. C. K. W. TAM and F. Q. Hu 1989 *Journal of Fluid Mechanics* **201**, 447–483. On the three families of instability waves of high-speed jets.
- 11. P. Mungur and G. M. L. Gladwell 1969 *Journal of Sound and Vibration* **9**, 28–48. Acoustic wave propagation in a sheared fluid contained in a duct.
- 12. S.-H. Ko 1972 *Journal of Sound and Vibration* 22, 193–210. Sound attenuation in acoustically lined circular ducts in the presents of uniform flow and shear flow.

- 13. A. E. GILL 1965 *Physics of Fluids* **8**, 1428–1430. Instability of top-hat jets and wakes in compressible fluids.
- R. J. Briggs 1964 Electron-stream Interaction with Plasmas. Cambridge, Massachusetts: MIT Press.
- 15. F. Q. Hu 1993 *Physics of Fluids* **5**, 1420–1426. A numerical study of wave propagation in a confined mixing layer by eigenfunction expansions.
- 16. C. K. W. TAM and T. D. NORUM 1992 American Institute of Aeronautics and Astronautics Journal 30, 304–312. Impingement tones of large aspect ratio supersonic rectangular jets.
- 17. C. K. W. TAM, K. A. AHUJA and R. R. Jones III 1994 American Institute of Aeronautics and Astronautics Journal 32, 915–922. Screech tones from free and ducted supersonic jets.